A Detailed Photometric Analysis of Early-Type Spiral Galaxies in Pairs

Miranda R. Gorsuch
University of Wisconsin – Stevens Point

Abstract

This project explores the relative role of "nature versus nurture" (intrinsically versus environmentally driven influences) in shaping the morphology and evolution of galaxies by performing a detailed photometric analysis of early-type spiral galaxies found in galaxy pairs. We use Fourier analysis to model the properties of the spiral arms and bulge/disk/bar decomposition analysis to find the properties of the bulge, disk, and bar of each spiral galaxy within our sample. We investigate the effect environmental density has on the formation and evolution of early-type galaxies by comparing our results with previous work done for samples of early-type galaxies found in different environments (isolated and loose groups). This analysis will allow us to gain more insight into the formation and evolution of spiral galaxies across a range of environments.

1. Introduction

The morphology of spiral galaxies remains an interesting study for extragalactic evolution, especially within a "nature versus nurture" context. This context focuses on the distinction of galactic evolution from the internal "nature" of an individual, lone galaxy versus a galaxy being "nurtured" by interactions with a neighboring galaxy.

This specific study focuses on spiral galaxies found in pairs. The spiral galaxy types are limited to early-type spiral galaxies with S0a, Sa, and Sab morphological classifications (n=17), including barred galaxies. High quality CCD images of this sample of galaxies are sourced from SDSS DR16 (Sloan Digital Sky Survey/Data Release 16; Ahumada et al. 2019). Different components of a galaxy's image require different analyses. The spiral arms of the galaxies are studied using Fourier decomposition, while the software BUDDA (**Bu**lge/**D**isk/bar **D**ecomposition **A**nalysis; de Souza 2004) is used to study the bulge, disk, and bar components of each galaxy. The Fourier and BUDDA analysis are done in both the *i*- and *g*-bands. Color analysis with the decomposed galaxy bulges depends on performing the BUDDA analysis in both bands, while visually confirming structures through the Fourier analysis is easier with two bands.

The sample of galaxies found in pairs is meant to compliment and bridge the gap between previous environments studied, where specific catalogues are used in order to easily group the galaxies based on their environment. This study utilizes the CPG (KPG) catalogue (**C**atalogue of Isolated **P**airs of **G**alaxies; Karachentsev 1972). The CPG catalogue implements isolation parameters, requiring that the typical latest outside interactions occurred at least one billion years ago (Domingue 2005). This requirement is vital in ensuring that there is a clear difference between secular evolution of galaxies versus changes brought about by interactions with their celestial partner. The same isolation parameter is also used in one of the samples used in previous studies. The CIG catalogue (**C**atalogue of **I**solated **G**alaxies; Karachentseva 1973) is ideal for showcasing isolated evolution of a single galaxy. To turn to a sample that looks more closely at more active galactic interactions, these previous studies used the **L**yon **G**roups of **G**alaxies (LGG) catalogue (Garcia 1993), which contain loose groups of 4-10 galaxies.

Two previous studies are specifically used to compare environments along with this project's CPG sample. Both of these studies used two samples of galaxies: isolated CIG galaxies (n=20 galaxies) and LGG group galaxies (n=39). Hess (2016) uses the BUDDA software package to decompose and record the properties of the bulge, disk, and bar for each spiral galaxy, while the second study, Hess (2017), performed a Fourier analysis for the same samples. These CIG and LGG samples are referenced throughout this paper as such.

2. Methods

This section describes the methods used for the detailed photometric analysis: BUDDA decomposition and Fourier analysis. Also described is the sample selection for this project and the method of analysis for the bulge colors after the BUDDA decomposition is performed.

2.1 Sample selection and preparation The criteria for the CPG sample selection is designed to align with the previous studies done with the CIG and LGG samples. For consistency, images must be available in the SDSS database. The recession velocity must fall between 1500 and 5000 km/s. This is to prevent the Local Group galaxies from being included in the sample, while ensuring that the galaxies fall close enough to do detailed photometry. The inclination of galaxies is limited for similar photometric reasons, where the inclinations greater than 70 degrees were excluded (the closer to face-on, the better). The galaxies chosen then must fall under an S0a, Sa, or Sab morphology classification, including barred morphologies. Once the CPG sample is finalized, images are downloaded from the SDSS DR16 database. All images are then cleaned using IRAF (Image Reduction and Analysis Facility) to remove the background stars.

2.2 BUDDA decomposition and analysis Once the images are cleaned of background stars, they are analyzed using the BUDDA software. The software, when inputted with an initial image and parameters, will fit a model for the galaxy's bulge, disk, and bar and output the image models and final parameters. There are two main equations that make up this model. The first shown as

$$I(r) = I_o e^{-r/h_R}, \qquad (1)$$

where $I(r)$ describes the intensity as a function of the radius, I_o is the central intensity, and h_R is the radial scalelength for the disk. Eq. 1 is a simplified, exponential version of the Sérsic profile, where n = 1. This simplified version is what BUDDA uses to fit the light profile of the disk. The full Sérsic profile is used to model the bulge and the bar, such that

$$I(r) = I_e 10^{-b_n[(r/r_e)^{1/n}-1]}. \quad (2)$$

With the full Sérsic profile, $I(r)$ remains the same as Eq. 1, I_e is the effective intensity, r_e is the effective radius, n is the Sérsic index, and b_n is a constant dependent on n. In this case, the effective radius is defined as the radius that contains half of the light of the bulge, with the effective intensity corresponding to the light contained within r_e.

The BUDDA decomposition is performed for each CPG galaxy image in both the i- and g-bands. This project honed in on a smaller number of parameters from the decomposition, focusing primarily on the attributes of the bulge given by the fit, such as its effective radius, Sérsic index, and luminosity.

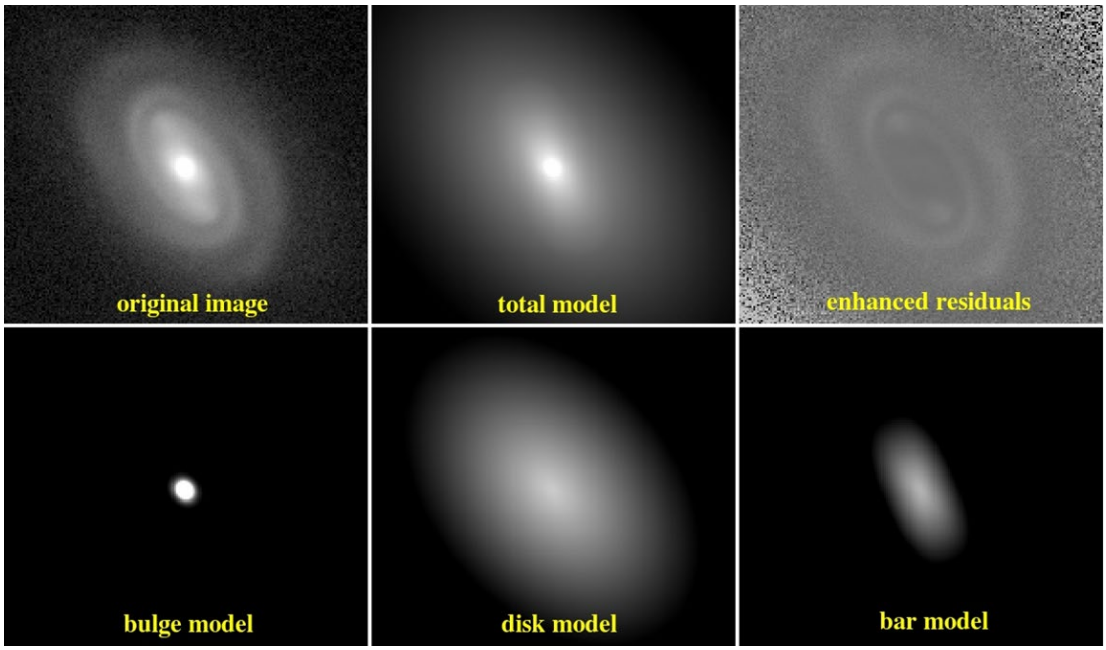

Figure 1: The figure above shows an example of a bulge/disk/bar decomposition of a barred galaxy. This model specifically shows CPG 303B in the *i*-band. The three models of the bulge, disk, and bar compose the total model.

2.3 Colors The color of the bulge is revealed by taking the apparent magnitude in the *g*-band and subtracting from it the apparent magnitude in the *i*-band (blue minus red). This process requires data from the BUDDA decomposition in order to separate the amount of light coming from the bulge. The apparent magnitudes are derived from the flux of the bulge model, which is provided by the BUDDA decomposition, measured within a radius that corresponds to a surface brightness of 24 mag arsec^{-2} in the *i*-band. The apparent magnitudes are corrected for galactic and internal extinction. Galactic extinction is applied using *extinction* parameter data from SDSS. Internal extinction corrections are performed using formulas for *g*- and *i*-band filters in Shao et al 2007, where *expAB* parameter is from SDSS.

An offshoot of doing color analysis is looking at the bulge concentration. The concentration used in this project is described in Durbala 2008, where C_{24} = 5 * log10(r80/r20), with C_{24} describing the concentration of flux from the bulge. The radius which contains 80% of the total flux of the bulge out to a surface brightness of 24 mag arcsec^{-2} in the *i*-band is divided by the radius which contains 20% of the flux. For this project, the C_{24} was only calculated in the *i*-band, due to likely similar results in the *g*-band (though a future project can be done to confirm the results in the *g*-band).

2.4 Fourier analysis The galaxy images removed of background stars are deprojected into circles within IRAF using the position angle of the galaxy within the image and ellipticity parameters found through the BUDDA decomposition within the *i*-band. Once the deprojected images are generated, they're run through the Fourier decomposition. With this decomposition, the light from the galaxy is modeled as a light distribution expanded using a Fourier series in polar coordinates (Durbala 2009). This Fourier series can be written a couple different ways, either as

$$I(r,\phi) = I_0(r) + \sum_{m=1}^{\infty} I_{mc} \cos m\phi + \sum_{m=1}^{\infty} I_{ms} \sin m\phi, \quad (3)$$

or

$$I(r,\phi) = I_0(r) + \sum_{m=1}^{\infty} I_m(r) \cos[m(\phi - \phi_m)]. \quad (4)$$

In both Eq. 3 and Eq. 4, $I_o(r)$ represents the azimuthally averaged intensity in a circular annulus of radius r on the galaxy plane. I_{mc} and I_{ms} respectively represent the cosine and sine amplitudes, while ϕ_m is the phase for each Fourier component m. In addition, the Fourier I_m amplitudes are expressed by

$$I_m = \sqrt{I_{mc}^2 + I_{ms}^2}. \quad (5)$$

The Fourier term m corresponds to the number of spiral arms in a set. For example, a galaxy with two main spiral arms will have a dominant term of $m = 2$ and may also have less obvious m terms that can be revealed using a numerical analysis. The numerical analysis (the Fourier decomposition) provides the initial guidance on the shape of these less obvious terms, which are then considered dominant when they are visually confirmed in the original image in both bands. The previous galaxy example may then have a set of three spiral arms that are more subtle compared to the main set of $m = 2$ arms. This galaxy may then be assigned both $m = 2$ and $m = 3$, which is shortened to $m = 2 + 3$.

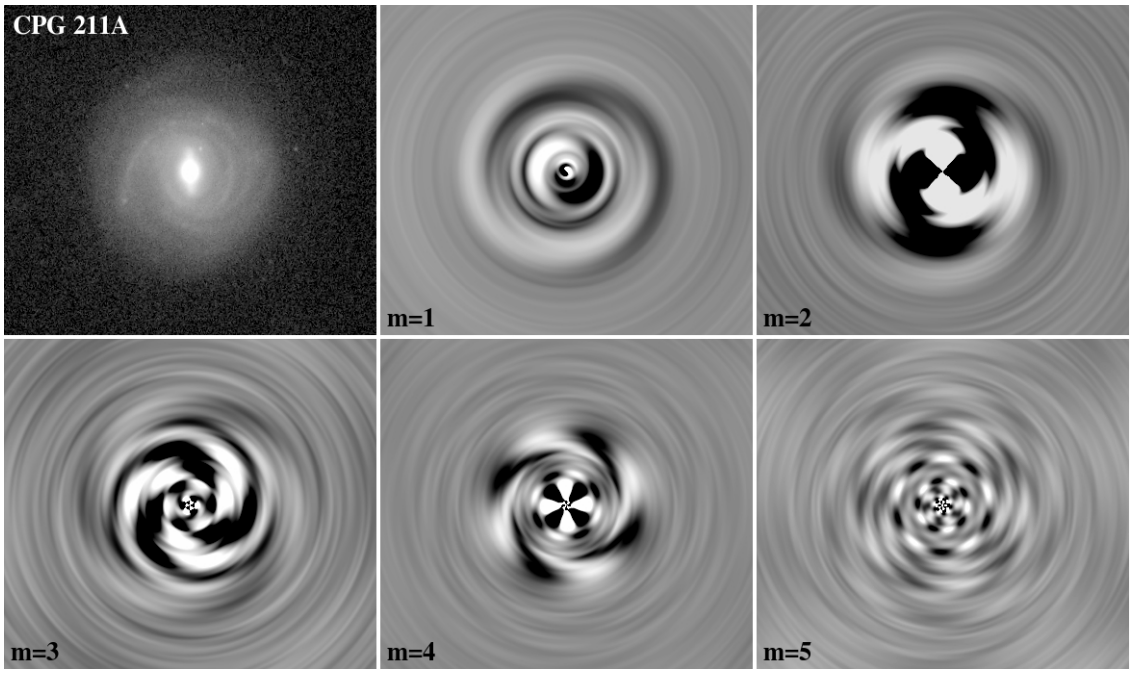

Figure 2: This figure shows an example of a Fourier decomposition of the galaxy CPG 221A with its *i*-band image. All terms from 1-5 are shown. The dominant terms for this galaxy are m = 1, 3, and 4.

The Fourier decomposition example in Fig. 2 shows the original galaxy image in the *i*-band, and the resulting Fourier terms up to $m = 5$. Note that the dominant terms are $m = 1$, 3, and 4. Although an example from the *g*-band is not shown, dominant terms are confirmed visually in both bands.

3. Results

This project has utilized two main methods for the analysis of galaxy morphology: BUDDA decomposition for the bulge, disk, and bar, as well as some color analysis, while the Fourier analysis focuses on the spiral arms. With the methods described, the results can now look at comparisons to the CIG (isolated) and LGG (group) samples analyzed in Hess (2016), and Hess (2017), respectively.

Combining the results of the BUDDA decomposition with the color analysis yields some interesting results. The first comparison of interest, seen in Fig. 3, is the effective radius of the bulge across the Sa samples, between the three environments. The CPG galaxies (those in pairs) are of note in this comparison due to r_e being significantly smaller than the other two environmental samples, with a median of 0.58 kpc for CPG compared to 0.80 and 0.94 kpc for the CIG and LGG samples, respectively.

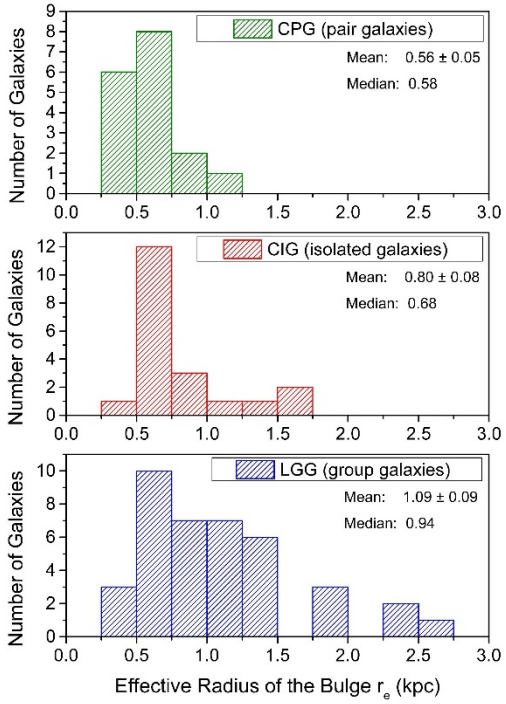

Figure 3: This figure shows a histogram of the effective radius of the bulge, r_e, between the three Sa environmental samples. The comparison of r_e indicates the CPG sample tend to have smaller bulge sizes.

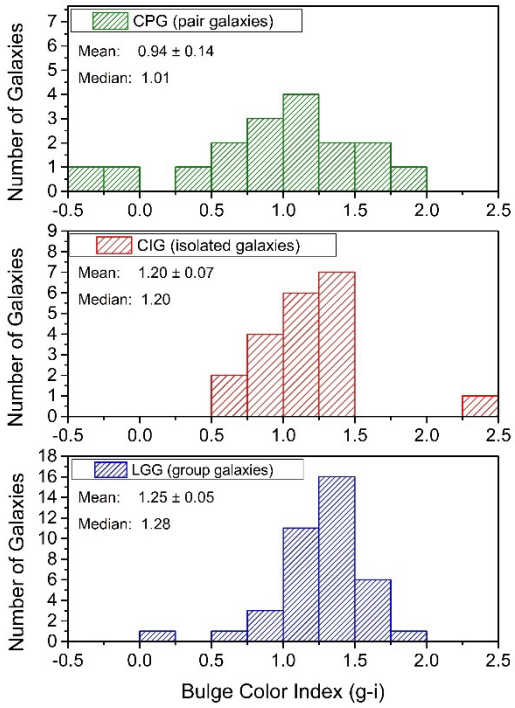

Figure 4: The figure above shows a comparison of the bulge color index for each sample. The CPG sample occurring with bluer bulge colors than the isolated and loose group samples.

Another comparison, seen in Fig. 4 is the color index of the bulge (*g-i*). Again, the CPG sample stands out from the other two, in that the bulge colors tend to run bluer. The CPG sample shows a color index median of 1.01 (lower numbers being bluer), while the CIG sample shows a 1.20 median, and the LGG sample a 1.28 median.

Figures 5 and 6 show more comparisons between parameters of the bulge. Fig. 5 shows a linear correlation between the absolute magnitude of the bulge and r_e of the bulge. The CPG sample leans

towards the lower end of both parameters, showing that the isolated pairs tend to have less luminous and smaller bulges. Fig. 6 shows that the CPG bulges tend to have lower concentration, as well as smaller values for their Sérsic indices.

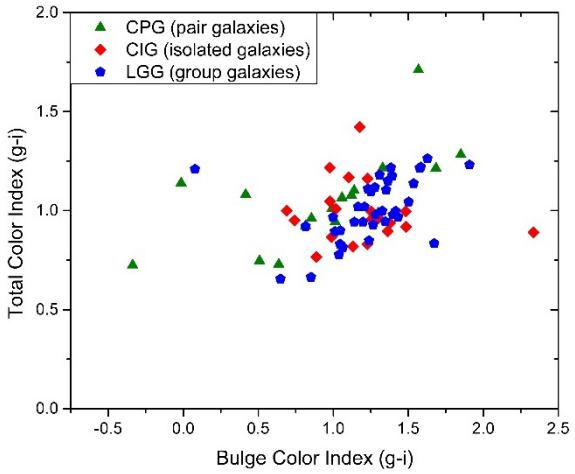

Figure 5: The CPG sample shows consistency with the CIG and LGG samples by displaying an expected linear correlation between the bulge size and luminosity. CPG galaxies tend to have smaller and less luminous bulges.

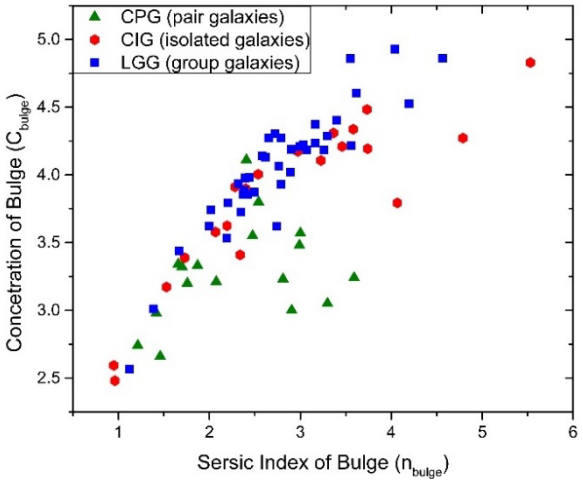

Figure 6: The CPG sample follows the correlation shown by the CIG and LGG samples, showing that a bulge with larger Sérsic index tends to have a large concentration. Bulges of CPG galaxies tend to have lower values of C_{24} and the Sérsic index.

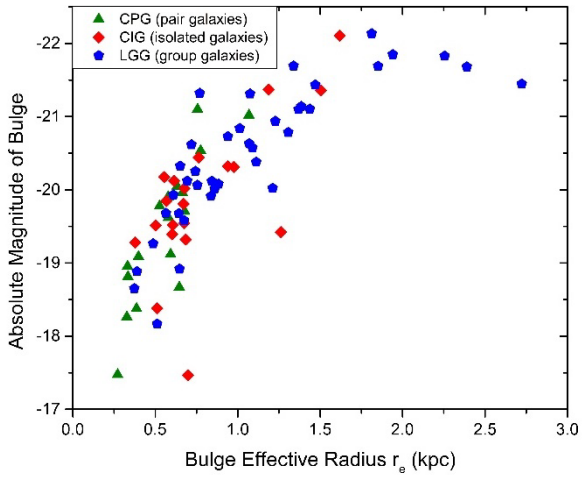

Figure 7: Shown in this graph is the overall color of the galaxy compared to the color of the bulge. There is generally a linear correlation between the bulge and total color. This plot shows that the CPG sample tends to have bluer bulges, but CPG total color is consistent with the CIG and LGG samples.

Fig. 7 shows the total color index of the galaxy (all of the galaxy's light) versus the color index of the bulge. The total color indices (*g*-*i*) for the three early-type samples remain similar. The mean / median for the CPG, CIG, and LGG samples (in order) are the following: 1.05 / 1.06, 0.99 / 0.96, and 1.16 / 1.00. For the most part, there is a loose linear correlation between these two color indices, however the CPG is again shown to tend toward the bluer end for the bulge, but overall maintains a similar total color index as the CIG and LGG samples.

A final parameter to note, with no companion figure, is the luminosity ratio L_{bulge} / L_{total} for the early-type galaxies. The CPG ratio comes to 0.28 / 0.24 (mean / median), the CIG with a 0.22 / 0.22, and the LGG with a 0.28 / 0.26. These are all fairly similar, an expected result as these three samples all fall under the same morphological category.

The results of the Fourier analysis are relatively straightforward and summarized in Fig. 8; this analysis now includes late-type samples (Sb's) from the CIG and LGG catalogues in Hess (2018). The Fourier term $m = 2$ is the dominant term for all morphological types and environments, appearing in about 35% for late-types and 60% for early-types. This difference appears to rely on morphological type rather than the environment. This morphological preference is again shown for the $m = 2 + 3$ (a set of two and a set of three arms); this combined term appears in about 27% of late-types, and only 10% of early-types. The LGG Sa sample has no galaxies with $m = 2 + 3$, while the CIG Sa and CPG Sa have 9.5% and 11.8%, respectively. Meanwhile, the $m = 1 + 2$ combined term has a consistent range of 10-20% for both early and late-types. The LGG Sa sample leads with the highest amount with 22.5% of galaxies showing this combination of dominant terms.

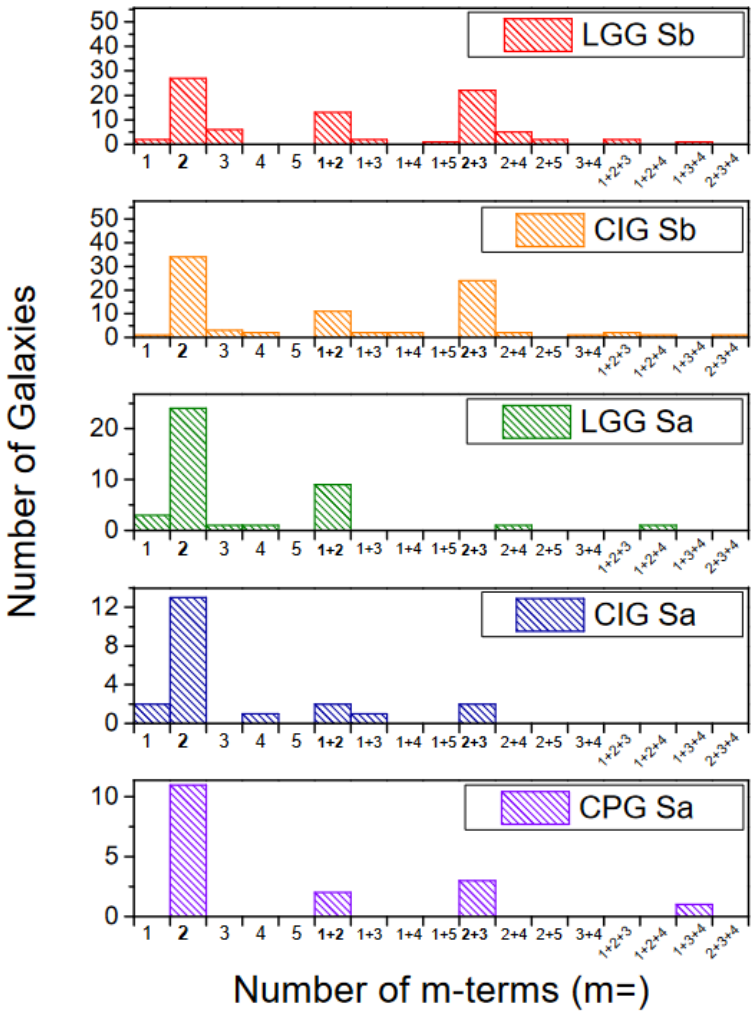

Figure 8: The figure above is the compiled results of the Fourier decomposition analysis. The most common dominant term across all sample types is the $m = 2$ term, which appears approximately twice as often in early-types than in late-types. The combined term $m = 2 + 3$ appears ~3x as often in late-types than early-types, while the third most common term of $m = 1 + 2$ remains in a consistent range of 10-20% for both morphological types. The difference in occurrences seem to depend on morphological type rather than the environment.

	n	% total
LGG Sb	4	4.8
CIG Sb	2	2.3
LGG Sa	9	22.5
CIG Sa	2	9.5
CPG Sa	1	5.9

Table 1: The number of galaxies with counterwinding terms for several examples across morphological and environmental type. Counterwinding galaxies appear significantly more often in early-type (Sa) galaxies, the majority belonging to LGG Sa types. Counterwinding terms indicate recent mergers between galaxies.

An interesting phenomenon with Fourier decomposition is the appearance of counterwinding, where two sets of spiral arms wind in opposite directions. As counterwinding arms are unstable structures, they fade relatively quickly, and indicate recent mergers through outside interactions (an example of nurture). When several samples are compared in terms of morphological type and environment, early-type galaxies (Sa's) show the greatest number of counterwinding terms. The largest amount belongs to the LGG Sa sample (22.5 %), more than twice the amount of the next largest sample (CIG Sa, 9.5%). The LGG Sa sample having the largest number of counterwinding galaxies is in line with expectations, as there are plenty of opportunities for interactions between neighboring galaxies.

4. Discussion

Comparing the CPG sample to the LGG and CIG studies revealed confirmations along with interesting divergences between the environments. The Fourier analysis with the CPG sample aligns with the results of the CIG and LGG samples, where the Fourier term $m = 2$ remains the dominant term across all morphological types and environments, and the Fourier term $m = 1 + 2$ is still the most common within the LGG Sa sample. It's reasonable seeing the loose group environment hosting the largest amount of counterwinding appearances to assume that more neighboring galaxies implies more interactions resulting in residual counterwinding. However, there's an interesting implication of the counterwinding appearing more prevalent in the isolated Sa sample than the paired Sa sample. The assumption that the CPG sample will show more examples of counterwinding due to a neighboring galaxy is no longer strongly supported, and instead could possibly suggest that the isolated galaxies are isolated due to recently merging with a neighboring galaxy.

The BUDDA decomposition method used in this project is also used in the Durbala et al (2008) paper. The Hess 2018 comparison for Sb-Sc galaxies presented in this paper uses a sample of 97 late-type Sb/Sbc/Sc spiral galaxies from the CIG/AMIGA (**A**nalysis of Interstellar **M**edium of **I**solated **G**alaxies) and analyzes the bulge, disk, and bar parameters, where the AMIGA sample is an updated version of the CIG catalogue. The results of this study found that the largest percentage of the pair sample show a Sérsic index between 1.3 and 1.4, while the majority still fell below n = 2.0-2.5. Note that lower values of the Sérsic index (n<2.5) indicate pseudobulges (disky), and larger values of the index indicate classical bulges (ellipsoidal); pseudobulges are mainly formed through secular evolution, while classical bulges mainly appear through mergers. The galaxies within the AMIGA Sb-Sc sample mostly host pseudobulges.

Now within the context of the CIG/AMIGA sample, it's interesting to note the differences of the CPG sample compared to the CIG and LGG samples while pointing out that pseudobulges are more "disky" (i.e. bluer in colors, smaller radii, lower Sérsic index) and indicate secular evolution. From the results section, it can be seen that the bulges in the CPG sample trend toward being bluer in color, smaller in radius, and having lower values of the Sérsic index. These three parameters

suggest that the CPG sample has more pseudobulges than the CIG and LGG samples. The presence of pseudobulges is usually associated with secular evolution. The larger number of pseudobulges in galaxy pairs combined with a low counterwinding parameter further indicates more "nature" than "nurture" affecting the evolution of the galaxies in the CPG sample than for the CIG and LGG galaxies. In terms of the nature vs. nurture context introduced at the beginning of this paper, the CPG sample indicates that galaxies found in pairs have been more likely to be evolving due to their internal structure compared to the other environment samples. These results also indicate that isolated galaxies may be more likely to be evolving from outside interactions than the CPG sample. Meanwhile, the LGG sample shows an expected high amount of evolution due to interactions with neighboring galaxies.

Despite the time intensive process, an increase in sample size - especially for the CPG sample with 17 galaxies - would be ideal. However, the sample size is limited by the selection process and the need to maintain the process in order to compare samples. A clear path to continue this project is to perform the BUDDA and Fourier decomposition on a CPG Sb sample. This would act as a natural way to fill the gap in environments for late-type galaxies as well as act as a work-around for increasing the sample size for pairs of galaxies.

5. Acknowledgments

The author would first like to thank Dr. Adriana Durbala for acting as the project advisor and offering her guidance through the years. The support of the Undergraduate ALFALFA Team was also essential for this project. The project itself was worked within the facilities of the University of Wisconsin – Stevens Point as the author's undergraduate institution, while the author's current institution is the University of Wisconsin – Madison.

The author would also like to acknowledge the generous support of WSGC and state that this material is based upon work supported by NASA under Award No. UGR21_4.0 issued through Wisconsin Space Grant Consortium. Any opinions, findings, and conclusions or recommendations expressed in this material are those of the authors and do not necessarily reflect the views of the National Aeronautics and Space Administration.

This study has made use of SDSS DR16. Funding for the Sloan Digital Sky Survey IV has been provided by the Alfred P. Sloan Foundation, the U.S. Department of Energy Office of Science, and the Participating Institutions. SDSS acknowledges support and resources from the Center for High-Performance Computing at the University of Utah. The SDSS web site is www.sdss.org.

SDSS is managed by the Astrophysical Research Consortium for the Participating Institutions of the SDSS Collaboration including the Brazilian Participation Group, the Carnegie Institution for Science, Carnegie Mellon University, Center for Astrophysics | Harvard & Smithsonian (CfA), the Chilean Participation Group, the French Participation Group, Instituto de Astrofísica de Canarias, The Johns Hopkins University, Kavli Institute for the Physics and Mathematics of the Universe (IPMU) / University of Tokyo, the Korean Participation Group, Lawrence Berkeley National Laboratory, Leibniz Institut für Astrophysik Potsdam (AIP), Max-Planck-Institut für Astronomie (MPIA Heidelberg), Max-Planck-Institut für Astrophysik (MPA Garching), Max-Planck-Institut für Extraterrestrische Physik (MPE), National Astronomical Observatories of China, New Mexico State University, New York University, University of Notre Dame, Observatório Nacional / MCTI,

The Ohio State University, Pennsylvania State University, Shanghai Astronomical Observatory, United Kingdom Participation Group, Universidad Nacional Autónoma de México, University of Arizona, University of Colorado Boulder, University of Oxford, University of Portsmouth, University of Utah, University of Virginia, University of Washington, University of Wisconsin, Vanderbilt University, and Yale University.

References

Ahumada et al. 2020, ApJS 249, 3

De Souza et al. 2004, ApJS 153, 411

Domingue et al. 2005, AJ, 129, 2579

Durbala et al. 2008, MNRAS 390, 882

Durbala et al. 2009, MNRAS 397, 1756

Hess, L, 2016, 15th Annual UW System Symposium for Undergraduate Research and Creative Activity held at UW – Stevens Point

Hess, L. 2017, 27th Annual Wisconsin Space Grant Annual Conference held at UW - La Crosse

Hess, L. 2018, UWSP COLS Undergraduate Research Symposium

Garcia, A.M. 1993, AAS 100, 475

Karachenstev, I. D. 1972, Commun. Spec. Astrophys. Obs. USSR, 7, 1

Karachentseva 1973, Astrofiz. Issled.-Izv. Spets. Astrofiz. Obs., 8, 3

Shao, Z. et al. 2007, ApJ, 659, 1159

Sulentic, J.W et al. 2006, A&A 449, 937

Tody, D. 1986, "The IRAF Data Reduction and Analysis System" in Proc. SPIE Instrumentation in Astronomy VI, ed. D.L. Crawford, 627, 733

Origin. 2003. OriginPro. OriginLab Corp., Northampton, MA. URL http://www.originlab.com